JOURNAL OF THE BALKAN GEOPHYSICAL SOCIETY, Vol. 5, No 2, May 2002, p. 35-46, 8 figs.

Exploration of chrome ore in Southwestern Turkey by VLF-EM

M. Bayrak

Geophysical Engineering Department, Istanbul University, Avcilar Campus, 34850 Istanbul, Turkey
E-mail: mbayrak@istanbul.edu.tr

(Received 21 May 2001; accepted 30 August 2001)

Abstract: *Geophysical exploration for chrome ore deposits is rather complicated, and integrated geophysical methods should be used. For an integrated data interpretation respective data sets has been collected from VLF-EM ("Very Low Frequency"-electromagnetic), induced polarization (IP), gravity, magnetic and self potential (SP) data in southwestern Turkey. This area is known for its occurrence of chrome ore. VLF-EM parameters such as the apparent resistivity, phase, real and imaginary components of the vertical magnetic field and tilt angle of the magnetic polarization ellipse were acquired using 16 kHz (GBR, Rugby, England) radio signal. Mapping of the VLF-EM resistivity, phase, real component of vertical magnetic field and filters (Fraser filter, 1969 and Karous and Hjelt filter, 1983) yields good results in distinguishing conducting ore bearing fault zones within the resistive ultrabasic rocks. The dominant feature of the reconnaissance mapping is that the low values of resistivities (<100 Ohm.m) extend in about N 25^{o} E direction. This characteristic direction correlated with the extension of known chrome occurrences in the field. Displaying of the VLF-EM real 2-D current density pseudosections along three profiles, secondary currents were followed with depth in the ground.*

Key Words: *Chrome Ore, VLF-EM, Integrated Geophysics, Southwestern Turkey*

INTRODUCTION

The application of VLF-EM survey for rapid and cost effective geological mapping and detection of subsurface conductive targets is a well established method that has been in use for over 30 years in the 15-30 kHz frequency band (Paterson and Ronka, 1971; Phillips and Richard, 1975, Fischer *et al*., 1983; McNeill and Labson, 1991; Ogilvy and Lee, 1991; Ogilvy *et al*., 1991; Tabbagh *et al*., 1991; Bayrak, 1993; Bayrak and Ilkisik, 1995; Guerin and Benderitter, 1995). Remote radio transmitters operating in 15-30 kHz frequency bandwidth provide a worldwide network of marine communication and navigation systems.

Akpas Mining Company, General Directorate of Mineral Research and Exploration (MTA) and Istanbul University have undertaken a collaborative research (for improving the detection of conducting zones). This paper presents the remarkable results obtained with the VLF-EM method to detect in distinguishing conducting ore bearing fault zones within the resistive ultrabasic rocks in southwestern Turkey. Other geophysical techniques, including induced polarization (IP), gravity, magnetic and self potential (SP) methods were also applied to the area.

The advantages of VLF-EM method are lightweight and inexpensive equipment design, speed of field operation, ease in equipment handling, and low overall operation cost (Paterson and Ronka, 1971). VLF-EM method has proved to be an effective exploration tool for quick mapping of the resistivity, phase and other VLF-EM parameters such as the real and imaginary components of the vertical magnetic field which they are contain valuable diagnostic information and tilt angle of the near surface features using only 5 m of electric dipole.

GEOLOGY OF THE STUDY AREA

Figure 1 shows the location of survey area and its simplified geology. The metamorphic core of the Menderes Massif lies in the north of the study area. In the south, there are thick layers of autochton Jurassic-Cretaceous limestone. The boundary is covered by Lycian Napes of about 3-4 km thickness. Survey area is located over a subduction zone, which extend from Crete to Rhodos islands. Chrome ore occurs in ophiolitic type rocks of this belt.

The chrome ore deposits are linked mainly to the upper part of a harzburgite-dunite-tectonite sequence, as well as to the lower part of a dunite cumulate sequence of ultramafic massifs. Most chrome-bearing deposits are of pediform type, less is stratiform. Dunides and harzburgites are often serpentinized and contain secondary magnetite in a fine-grained, disseminated form or thin veinlet. These orebodies occur as sparsely-to-densely disseminated, nodular, belted or massive chromes. The type of ore is chromespineled, mainly magnesian and sometimes ferrous. Its chemical composition is simple and the content of olivine and serpentine varies. In some cases the chrome grains are enclosed by secondary magnetite membranes, which are crystallized as a result of intense dynamic processes. Secondary magnetite is also present in chrome and serpentine. In Table 1, some of physical properties of chrome and ultramafic rocks are presented (Frasheri *et al*., 1995). The table shows that the resistivity values of chrome change from 700 to 3600 Ohm.m. If the ore is magnesian then the resistivity of ore can reach values less than 700 Ohm.m. In the Table 1, the dunite and harzburgite resistivity varies in the range of 2200 to 7000 Ohm.m. These are the most resistive from such kind of rocks. One of the noticeable point in the table is that, the serpentinized rocks are the most conductive and their resistivity vary from 35 to 100 Ohm.m. The chrome ore density is determined by the Cr_2O_3 content and, in general, a simple $\delta=40x+2000$ dependence is observed (Frasheri *et al*., 1995), where δ is the ore density in kg/m^3 and x is the percentage of Cr_2O_3 in the ore. This relationship is not unique, because the ore density is dependent on the degree of serpentinization of the olivine and also on the microfissures. In the Table 1, also the density of chrome appears higher than serpentinite type rocks. Due to chemical and thermal remanent magnetization, some chrome ores are magnetic. In the Table 1 while the mode susceptibility of chrome appears small, the serpentinite rocks have high values of mode susceptibility.

Table 1. Some of physical properties of chrome ores and ultramafic rocks (Frasheri *et al*., 1995).

Sample	ρ [Ohm.m]		Density [Kg.m^{-3}]			Magnetic properties in x10^{-5} SI units					
						Susceptibility			Remanent Magnetization		
	Min	Max	Min	Max	Mode	Min	Max	Mode	Min	Max	Mode
Chrome	700	3600	2450	4380	3700	10	500 3000*	150 300	70	8100	2800
Dunite	2200	7000	2700	3340	3020	10	1000	250	10	900	150
Serpentized dunite	100	650	2600	2800	2700	40	3000	250	10	800	700
Harzburgite	2400	7100	2800	3300	3050	10	700	200	10	1300	100 500
Serpentized Harzburgite	120	680	2700	2900	2800	20	1000	400	10	100	250
Serpentinite	35	100	2240	2650	2550	10	8000	1100	10	70000	300
Pyroxinite	170	1800	2900	3200	3080	10	320	100	10	71000	150

* Ores with high content of secondary magnetite

The petrophysical properties of ultramafic rocks are mainly subject to the degree of serpentinization and the physical and mechanical conditions. For this reasons (see Table 1) density is most stable and thus, it is the typical property used to differentiate between chrome ores and ultramafic rocks. Thus, gravity is the basic method used in chrome exploration. The values of geophysical anomalies over orebodies depend on the physical contrast between the chrome and surrounding rocks.

The chrome deposits are of podiform type within our survey area; the ore grading varies from disseminated through modular to massive. The matrix of the chrome is serpentine, serpentinized harzburgite-dunite or, in some cases, tromolite and chlorite. The chrome bodies, though in places shapeless, are, in general, in the form of elongated, lenticular pode. The size of the individual pode varies from 1 to 2 m up to 50 m in length and the thickness part from 0.5 m to 7-8 m. Boundaries between chrome and surrounding rocks are mostly very sharp. Primary magnetic contact relations are, however, of very restricted occurrence. Both massive and disseminated chrome ore are often seen together but separated where the boundary is clear by a zone of mechanical disruption (Engin, 1969).

SURVEY DESIGN

The survey, carried out in 1994, consisted of combined VLF-EM, induced polarization (IP), gravity, magnetic and self potential (SP) surveys. The uncertainty in extent of chrome ore was an important consideration in selecting this survey area. VLF-EM data were collected using the Scintrex EDA-OMNI equipment. The instrument is microprocessor controlled and facilitates automatic tuning, digital data capture and signal stacking. The magnetic field is recorded by the three orthogonal coils mounted in a cylindrical housing with a pre-amp signal circuit and the electric field is measured perpendicular to the magnetic field with two probes in contact with the ground which are placed 5 m apart. The measurements of both electric and magnetic field components for three VLF-EM transmitters can be made rapidly. Its lightweight and its design make handling easy for a single operator can obtain all these measurements in 3-4 minutes.

VLF-EM measurements were obtained using GBR (16 kHz) VLF-EM transmitter in England. This station provided the H-polarization data (in H-polarization mode, the electric field being perpendicular to the geologic strike). VLF-EM measurements were performed on ten profiles and 289 site with a grid spacing of 5×10 m over a chrome ore. The Ayse Ocak chrome ore ($FeCr_2O_4$) managed by Akpas Mining Company and is located on a 550 m high hill near the Fethiye-MUGLA of southwestern Turkey. The maximum depth of body is approximately 90-100 m, and 1-1.5 m thick veins oriented in N 25^o E direction. The survey area covers a 90 x 150 m. The topographic relief is gently undulating and there are no man-made conductors in the area. Also the area is free of cultural noise.

IP and SP surveys were obtained by Akpas Mining Company and gravity and magnetic surveys are applied by General Directorate of Mineral Research and Exploration (MTA) in 230×140 m area using Worden type microgravimeter and Proton magnetometer with a grid spacing of 10×5 m. Necessary latitude, altitude, topographic and other corrections are applied using a mean density value of 2700 kg/m^3.

VLF-EM METHOD

VLF-EM method is an inductive exploration method and the orthogonal horizontal electric ($E_{X,Y}$) and magnetic field ($H_{X,Y}$) components are measured operating in the 15-30 kHz frequency range. In principle it is possible to use both the E-polarization and the H-polarization excitations if convenient transmitters exist. The ratio of horizontal electric or magnetic field to the vertical electric (E_Z) or magnetic field (H_Z) is known as the tilt angle of the magnetic polarization ellipse and expresses as

$$W = \frac{E_{X,Y}}{E_Z} or = \frac{H_{X,Y}}{H_Z}\text{, in degrees.} \qquad (1)$$

The apparent resistivity ρ_a and the phase angle ϕ between horizontal electric field and magnetic field of the subsurface may be defined as a function of frequency as

$$\rho_a = \frac{1}{\omega\mu_0}\left|\frac{\mathbf{E}_{Y,X}}{\mathbf{H}_{X,Y}}\right|^2 \text{ in Ohm.m, (Cagniard, 1953)} \qquad (2)$$

and,

$$\phi = \tan^{-1}\left[\frac{\mathrm{Im}(\mathbf{E}_{Y,X}/\mathbf{H}_{X,Y})}{\mathrm{Re}(\mathbf{E}_{Y,X}/\mathbf{H}_{X,Y})}\right] \text{ in degree} \qquad (3)$$

where ω is the angular frequency and μ is the magnetic permeability of free space. In homogeneous isotropic ground, ρ_a is the true resistivity and the phase angle is 45^o. The skin depth describes the depth of penetration of the electromagnetic plane waves propagation in a conducting medium and expresses as

$$d \approx 503\left(\frac{\rho}{f}\right)^{1/2} \text{ in meters,} \qquad (4)$$

where ρ is the resistivity of the medium and f is the exploration frequency in Hertz (Mc Neill and Labson, 1991). For a discussion of detailed mathematical background of VLF-EM method the reader is referred to Mc Neill and Labson (1991).

Fraser (1969) filter applied to the tilt angle of the magnetic polarization ellipse. The Fraser filter calculates horizontal gradients and smoothes the data to give maximum values over conductors that can then be contoured. Consequently, the plotted Fraser filter function becomes,

$$F_{2,3} = (M_3+M_4) - (M_1+M_2) \qquad (5)$$

which is plotted midway between the M_2 and M_3 tilt angle stations (Fraser, 1969).

Real component of the vertical magnetic field of the VLF-EM data was Karous and Hjelt (1983) filtered. The filtered data can be considered as representation of the secondary currents in the ground. This filter is expressed as,

$$F_0 = 0.102H_{-3} - 0.059H_{-2} + 0.56H_{-1} - 0.56H_1 + \\ + 0.059H_2 - 0.102H_3 \qquad (6)$$

where H_{-3} through H_3 are the original VLF data, and F_0 is the filtered result.

The basic principles of the IP, gravity, magnetic and SP methods are well known and need not concern us here.

VLF-EM SPECTRUM

The VLF-EM transmitting stations operate within a relatively small band of frequencies range (15-30 kHz). We generally used Rugby (GBR, England, 16 kHz), Criggeon (England, 19 kHz) and Oxford (GBZ, England, 19.6 kHz) VLF-EM radio stations, because these stations are rather stable. However, prior to VLF-EM measurements, the periodic maintenance and repairing times of transmitters in certain days or hours should be taken into account. The VLF-EM transmission spectra of various radio stations have been measured at the survey area in the frequency range of 15-30 kHz (Figure 2). The observed transmission in different frequencies of VLF-EM spectrum provides a source field with adequate intensity for scheduled investigations in southwestern Turkey.

RESULTS

VLF-EM maps

VLF-EM maps (Figure 3, 4 and 5) were obtained using GBR (Rugby, England, 16 kHz) transmitter for H-polarization mode (electric field is perpendicular to the strike direction). To locate 2-D (two-dimensional) structures H-polarization mode are more reliable and also the resistivity contrast is being more important in H-polarization mode than in E-polarization mode (electric field is parallel to the strike direction).

Figure 3a and 3b shows the apparent resistivity ρ_{XY} and phase ϕ_{XY} maps, respectively. In the Figure 3a, the red colour tones which correspond to low resistivity values less than 100 Ohm.m extend along in N 25^o E direction on the eastern of the grid area. In the Figure 3b, the red colour tones which correspond to relatively high phase values bigger than 40^o also support the N 25^o E direction zone. This characteristic direction of N 25^o E

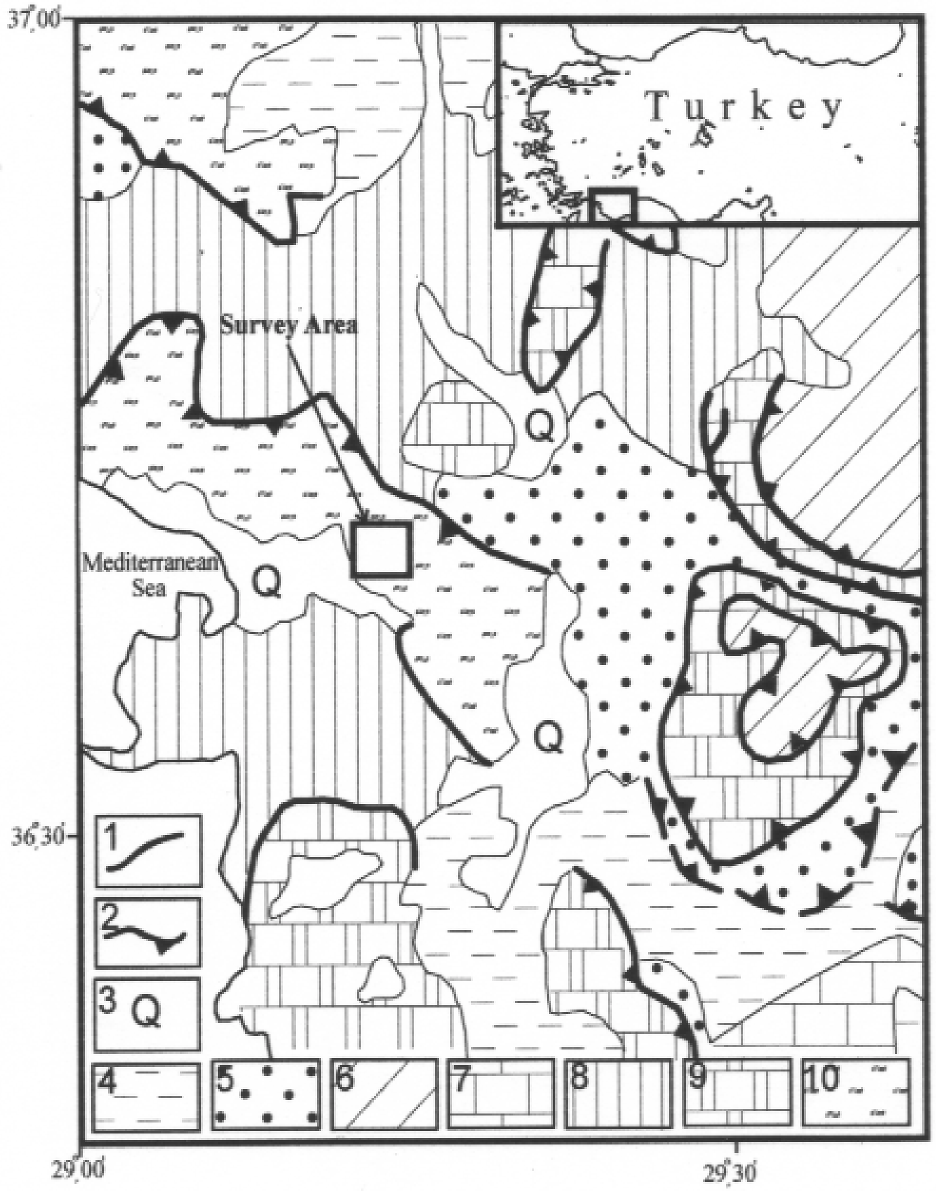

FIG. 1. Location and simplified geological map of southwestern Turkey; 1) Fault; 2) Overthrust; 3) Quaternary; 4) Neogene; 5) Eocene, flysch; 6) Triassic-Jurassic, melange; 7) Jurassic-Cretaceus, crystalline limestone; 8) Triassic-Jurassic, Limestone and dolomite; 9) Jurassic, limestone; 10) Peridodite and Serpentine (modified from General Directorate of Mineral Research and Exploration (MTA), 1964).

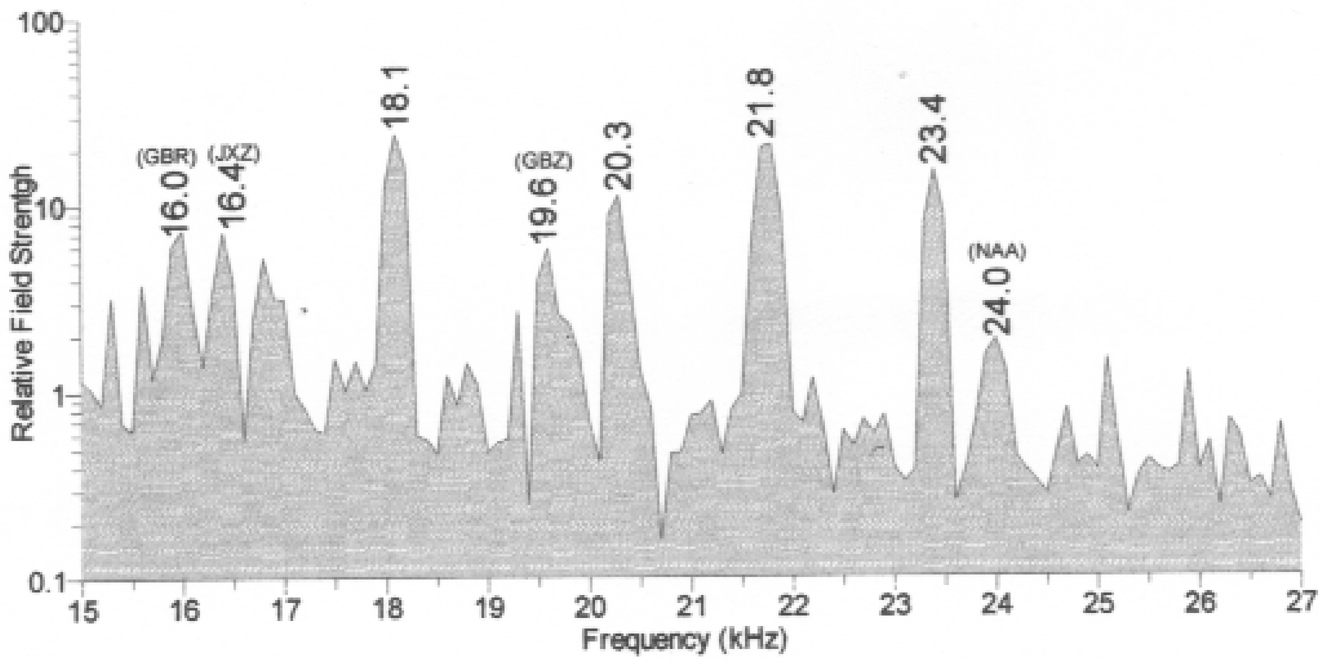

FIG. 2. VLF-EM spectrum measured in Fethiye, Mugla of southwestern Turkey on 10 August 1994.

correlates very well with the extending of a known chrome occurrence in the south end of field on the grid area. The similar extending anomaly that was followed in the middle of grid area, is more weak but this anomaly cannot be supported by the VLF-EM phase data.

Figure 4a and 4b show tilt angle of the magnetic polarization ellipse in degrees and Fraser (1969) filtered maps, respectively. In the Figure 4b, which is derived from Fraser (1969) filtering of the VLF-EM tilt data (upper map), it is quite clear that Fraser filtered values change its sign especially in around N 25^{o} E direction zone on the eastern of the grid area. This result is consistent with Figure 3. The sign changes in around N 25^{o} E direction zone shows conductive anomalies caused by serpentinized or mineralization zones.

Figure 5a and 5b show real component of vertical magnetic field (%) and Karous and Hjelt (1983) filtered maps, respectively. In the Figure 5b, I obtained a new map by applying Karous and Hjelt (1983) filter to the VLF-EM real component of vertical magnetic field data. Karous and Hjelt (1983) filter is an extension of the Fraser (1969) filter to process vertical component of magnetic field. Similar to the Fraser filter results, Karous and Hjelt (1983) filtered values change its sign in around N 25^{o} E direction zone on the eastern of the grid area. Areas with high ("-" signed) current density correspond to good conductors and conductive serpentinized zones. The resistive harzbugite and dunites zones are also clear. Again this filter result is consistent with both VLF-EM apparent resistivity and Fraser (1969) filter result taking the high negative current density values in around N 25^{o} E direction zone on the eastern of the grid area. It can be interpreted that if a conductive zone surrounded by relatively less resistive rocks then in this area mostly serpentinized type rocks located. In contrast, the conductive zones surrounded by very resistive rocks are possibly chrome ore or mineralization may occur within the dunite type rocks. A known chrome occurrence locates at the south end of N 25o E direction anomaly.

Figure 6 shows real component of vertical magnetic field and pseudosections of VLF-EM 2-D current density along L-8, L-5 and L-2 from (a) to (f). The locations of profiles are shown in the Figure 5a. In the all of pseudosections, the dominant features are high negative values that are representing by the red colour tones for investigation depth. The contact between the red and blue colour tones display zero value and this is important do determine chrome ore in the grid area.

IP, gravity, magnetic and SP maps

Figure 7a and 7b represent the metallic conduction factor (MF) and percent frequency effect (PFE) maps, respectively. High metallic conduction factor (>315) and high percent frequency effects (>2.3 %) values were represented with red colour tones in the figure. It is noticed that both MF and PFE anomaly maps perfectly resemble with VLF-EM apparent resistivity map. The characteristic N 25^{o} E direction anomaly can be followed with almost the same shapes both in MF and PFE anomaly map in consistent with to the VLF-EM parameters maps. The high MF values located in the northwestern part of the grid area plausibly reflect a conductive zone.

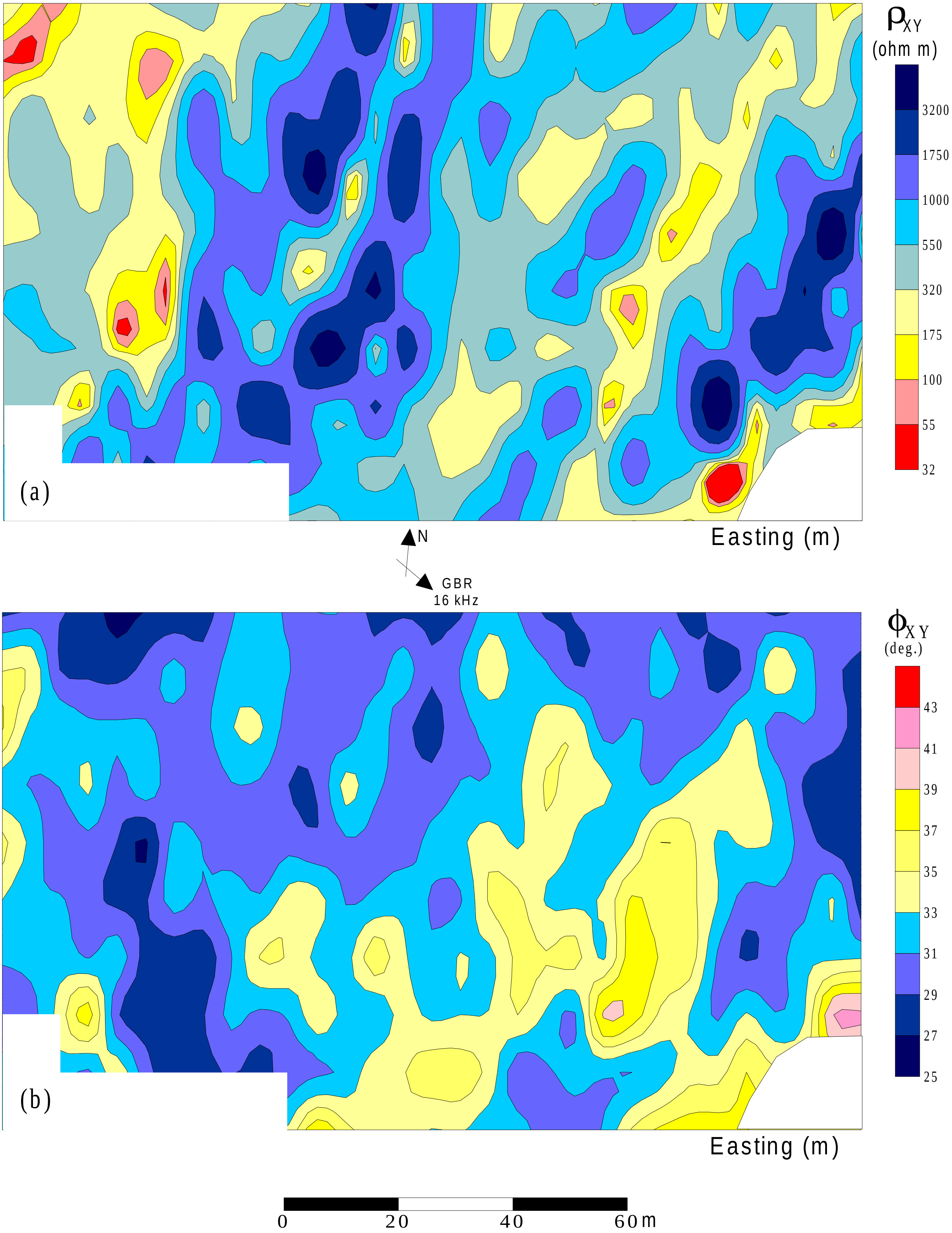

FIG. 3. (a) VLF-EM apparent resistivity (Ohm.m); (b) phase (deg.) contour maps for H-polarization mode: GBR transmitter (16 kHz, England). Arrow shows the direction of horizontal electric field.

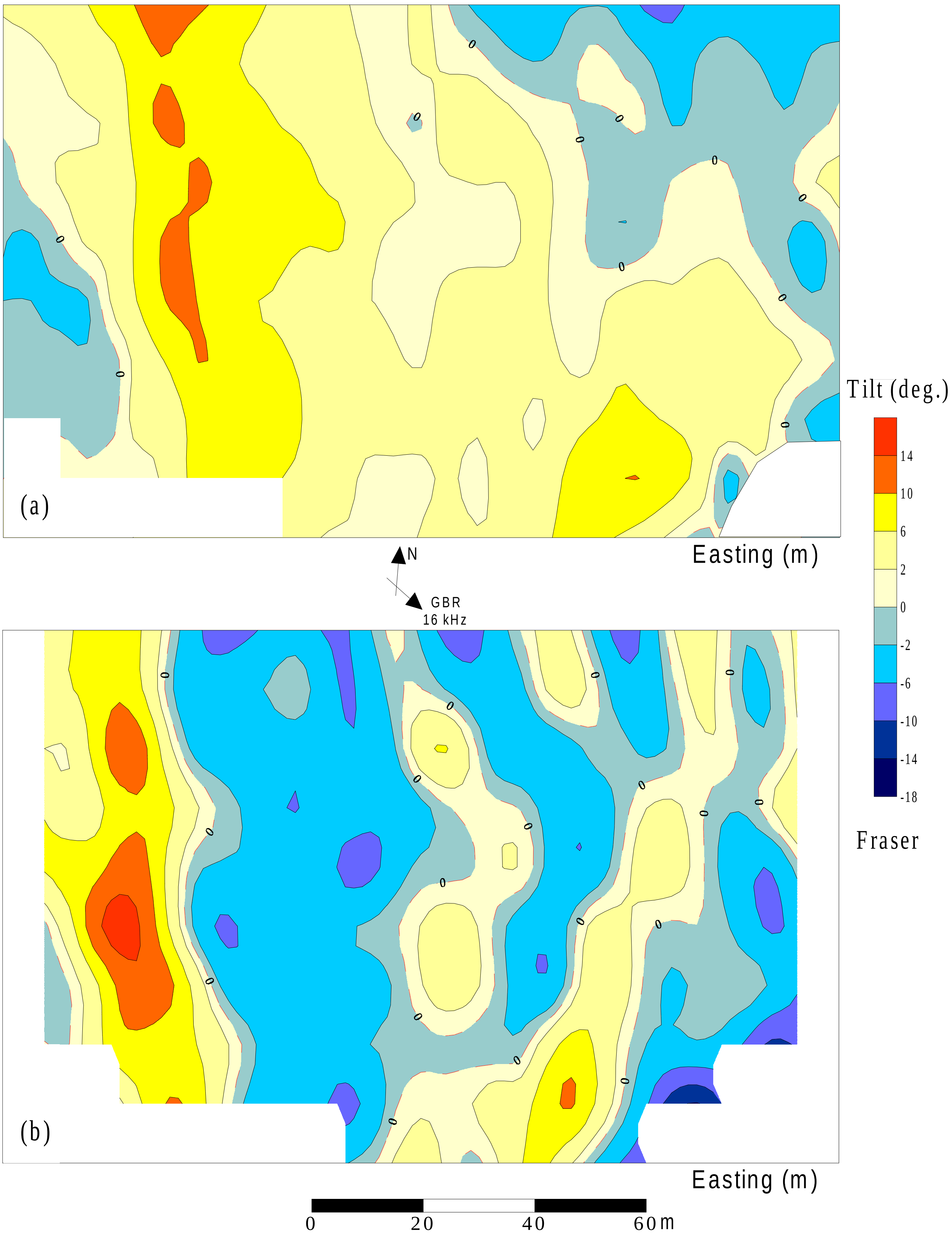

FIG. 4. (a) VLF-EM tilt angle of the magnetic polarization ellipse (deg.); (b) Fraser filtered contour maps for H-polarization mode: GBR transmitter (16 kHz, England). Arrow shows the direction of horizontal electric field.

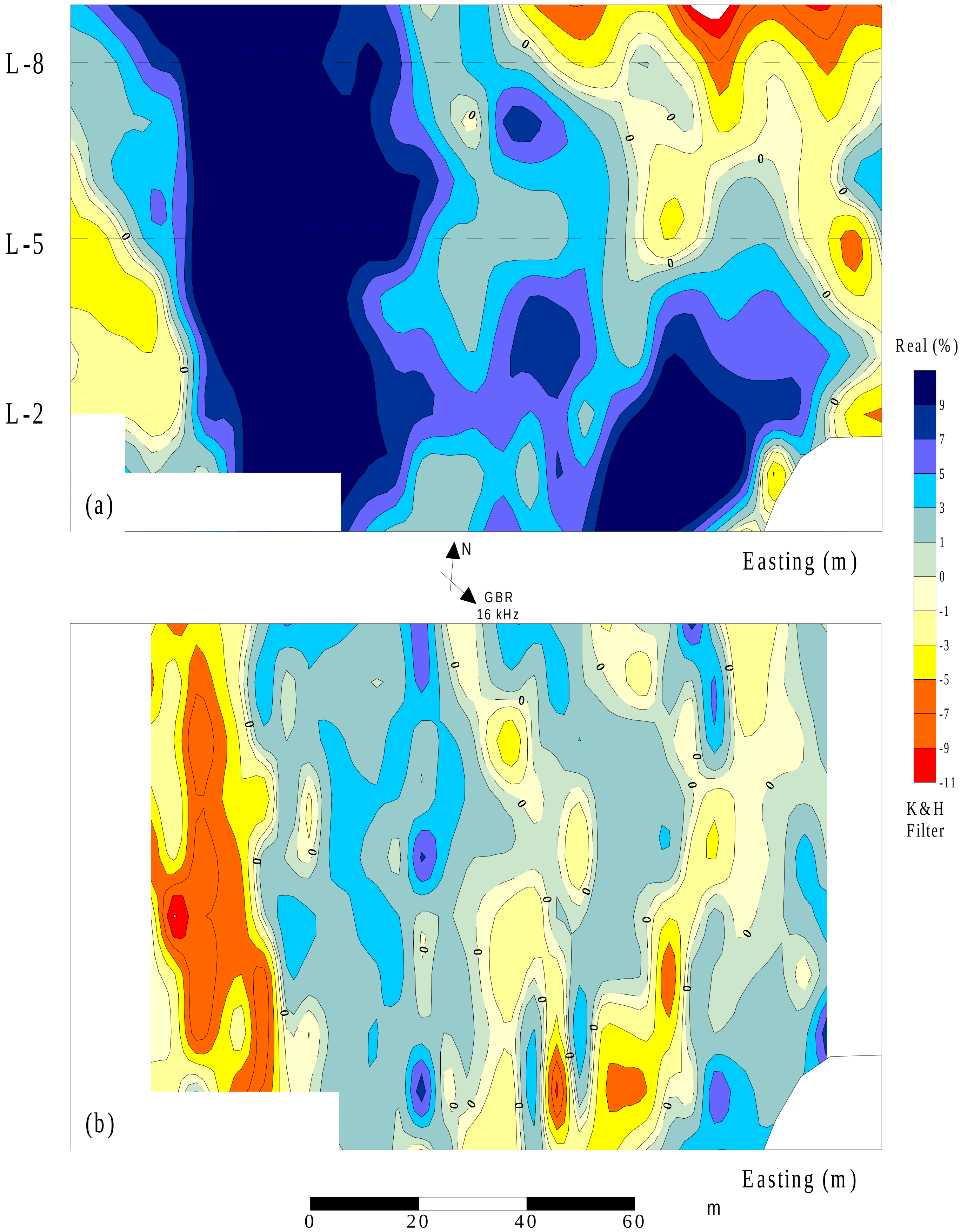

FIG. 5. (a) VLF-EM real component of vertical magnetic field (%); (b) Karous and Hjelt filtered contour maps for H-polarization mode: GBR transmitter (16 kHz, England). Arrow shows the direction of horizontal electric field.

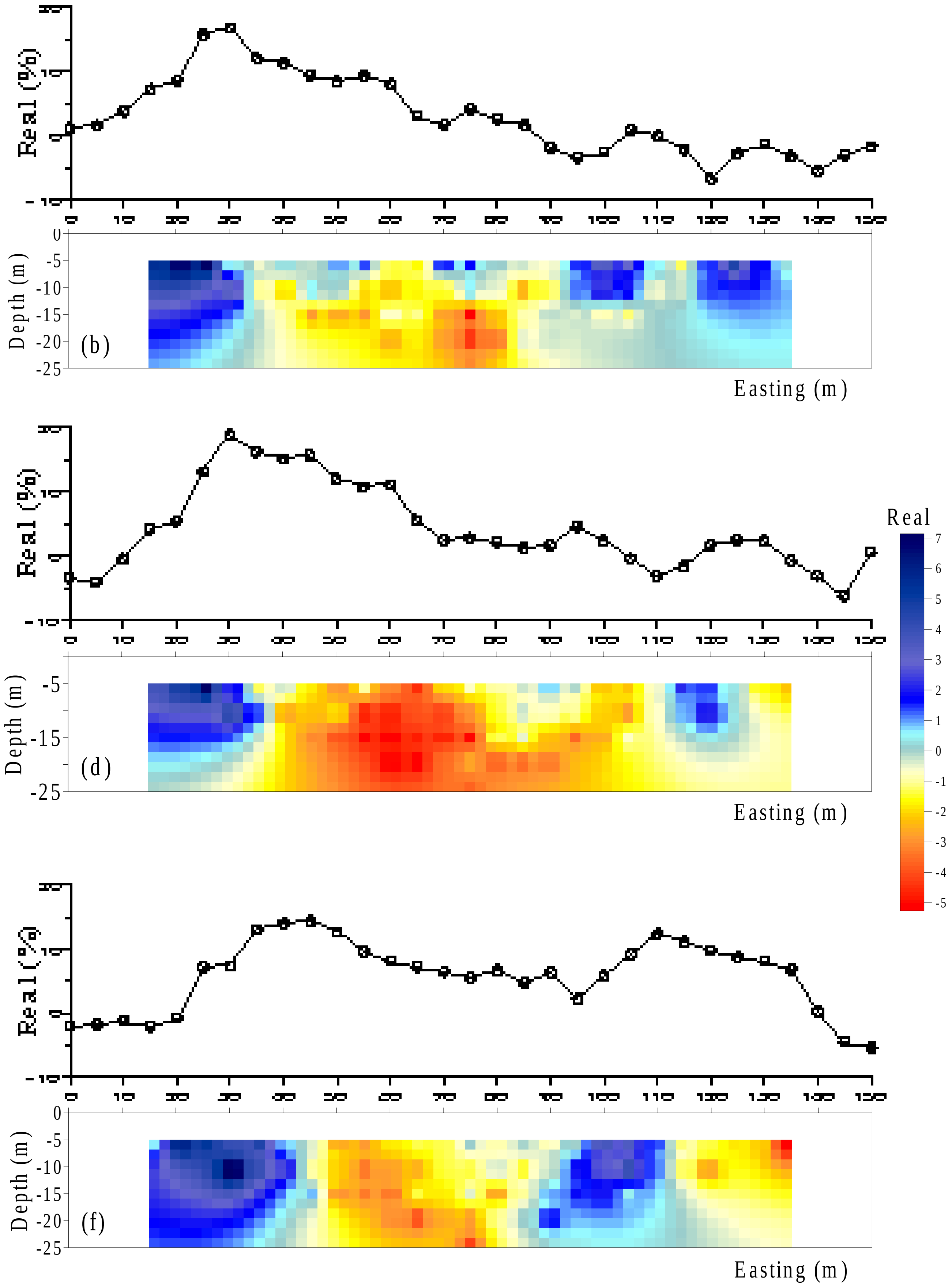

FIG. 6. VLF-EM real component of vertical magnetic field (%) and Pseudosections of 2-D current density along; (a-b) L-8; (c-d) L-5 and (e-f) L-2 profiles. The horizontal axis shows easting and vertical axis shows depth in meters.

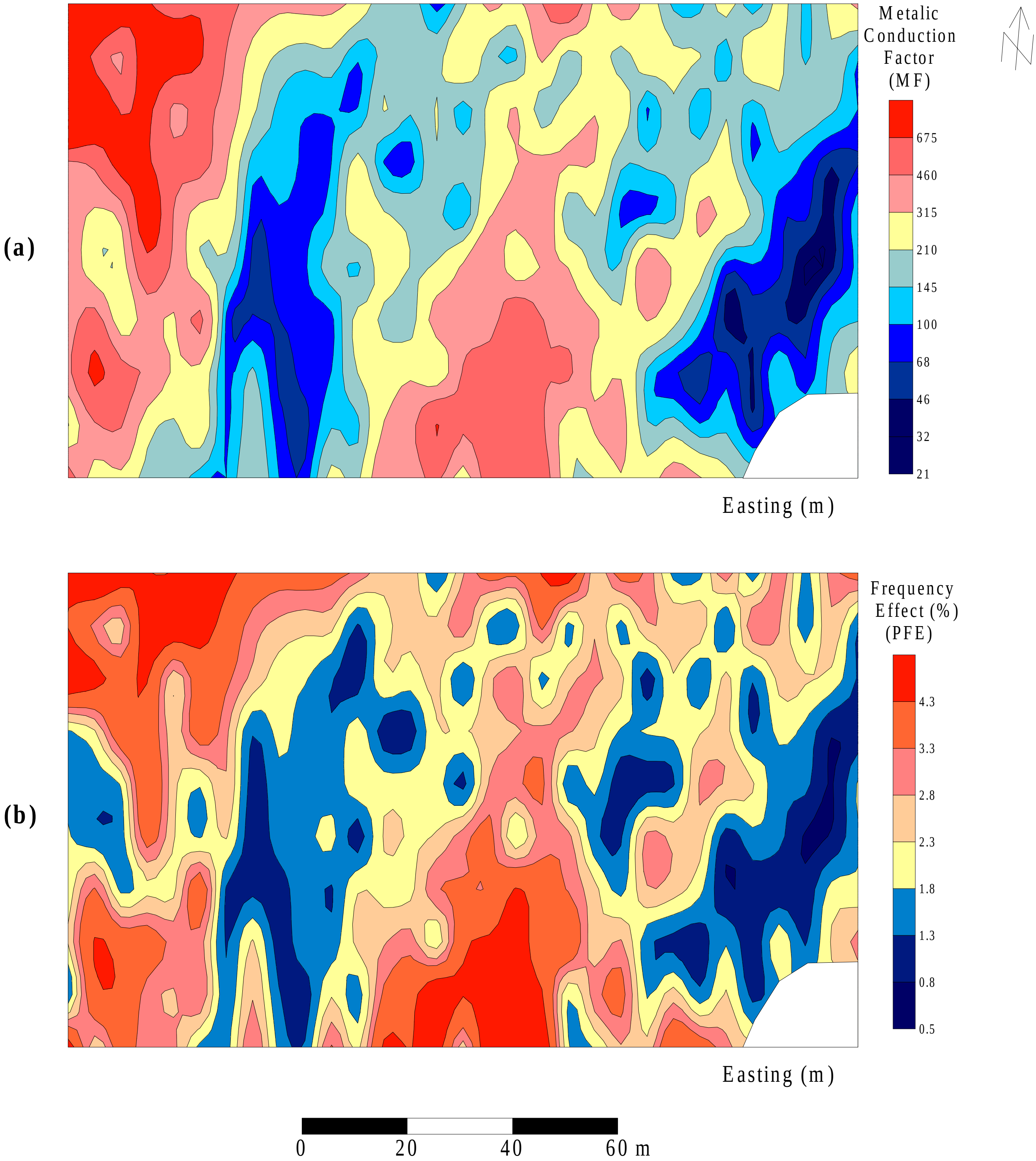

FIG. 7. (a) Induced polarization (IP) metallic conduction factor (MF); (b) percent frequency effect (PFE) contour maps.

Figure 8 (a) shows the total magnetic intensity anomaly in nT. Although, there are some positive magnetic anomalies sparsely distributed, this map gives not distinct information about mineralization. Only an anomaly appears in southeast corner of map, which locates on a known shallow chrome occurrence; (b) The Bouguer gravity anomaly is shown in milligals (mGal). The regional density variation increases from north to south direction. A local positive gravity anomaly about at the centre of survey area reflects the density of dunite type rocks surrounded by possibly serpentinized rocks; (c) The gradient of self potential values is shown in mV/m. The gradient array was used in this research. Although, the pattern of anomalies are not clear, we consider that northeast southwest oriented negative anomalies mostly fits with the conductive serpentinized zones.

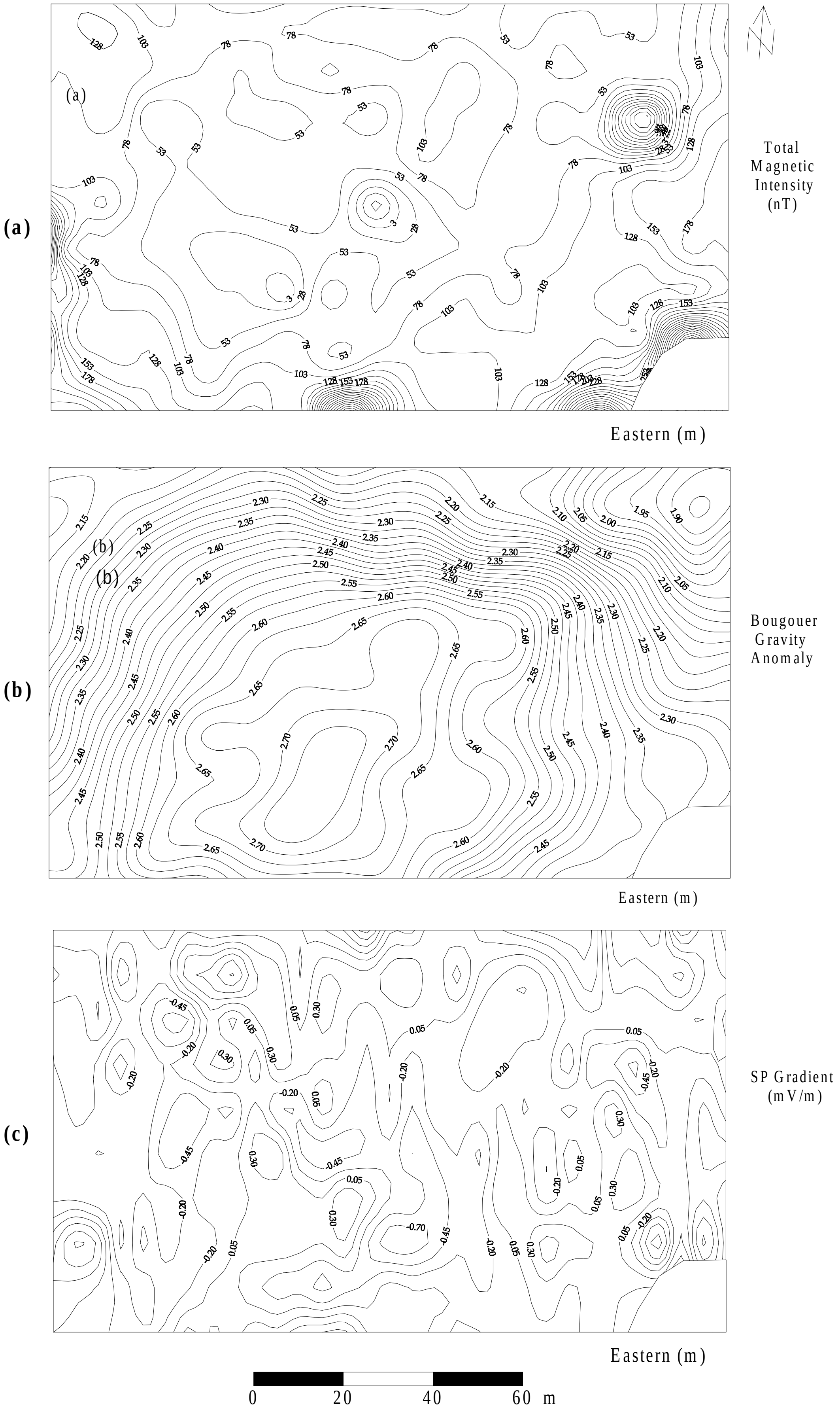

FIG. 8. a) Total magnetic intensity contour map in nT; b) Bouguer gravity anomaly contour map, contours are in mGal; c) Self potential gradient contour map in mV/m.

CONCLUSIONS

Combining the results of a VLF-EM survey with those of IP, gravity, magnetic and SP surveys provides an integrated evaluation of anomalies by detecting conducting zones effectively. VLF-EM method has been proved as a fast and cost-effective tool for mapping of chrome ores. The VLF-EM transmission spectra of various radio stations have been measured for the first time and founded having adequate intensity in southwestern Turkey. Apparent resistivity, phase and derived quantities such as Fraser (1969) and Karous and Hjelt (1983) filters show that there are several anomalies especially extending in about N 25^o E direction. Similarity between the VLF-EM apparent resistivity map and IP maps such as MF and PFE is interested in around N 25^o E oriented anomaly. These anomalies correspond to chrome mineralization in Dunit/Harzburgite type rock and serpentinized rock boundaries. N 25^o E characteristic direction is correlated with the extending of known faulted chrome occurrences in the study area. The geometry of chrome ore is controlled by lots of faults and a known chrome ore is located at the south end of this anomaly on the grid map. Our field studies suggest that the VLF-EM method can be used as a fast and inexpensive tool for mapping over chrome ores that are important for Turkish mining industry.

ACKNOWLEGMENTS

The author thanks O. Metin Ilkisik, who is principal execution of the project and Ates Adalan of Akpas Mining Company for initiating and directing of the project. Many thanks to Ilka Lahti of Ohulu University for his FORTRAN code. The paper is published with the permission of the Director, Akpas Mining Company.

REFERENCES

Bayrak, M., 1993. VLF measurements and interpretations (in Turkish): M.Sc. Thesis, Graduate School of Natural and Applied Sciences, Istanbul University, Istanbul, Turkey.

Bayrak, M. and Ilkisik, O.M., 1995. Use of electromagnetic-VLF method in shallow explorations in Turkey (in Turkish): Jeofizik, **9-10**, 143-148.

Cagniard, L., 1953. Basic theory of the magneto-telluric method of geophysical prospecting: Geophysics, **18**, 605-635.

Engin, T., 1969. The geology and geochemistry of the ultrabasic rocks and associated chrome deposits of the Andizlik-Zimparalik area, Fethiye, southwest Turkey: Ph.D. Thesis, University of Durham.

Fischer, G., Le Quang, B.V. and, Müller, I., 1983. VLF ground surveys, a powerful tool for the study of shallow two-dimensional structures: Geophysical Prospecting, **31**, 977-991.

Fraser, D. C., 1969. Contouring of VLF-EM data: Geophysics, **34**, 958-967.

Frasheri, A., Lubonja, L, and Alikaj, P., 1995. On the application of geophysics in the exploration for copper and chrome ores in Albania: Geophysical Prospecting, **43**, 743-757.

Guerin, R., and Benderitter, Y., 1995. Shallow karst exploration using MT-VLF and DC resistivity methods: Geophysical Prospecting, **43**, 635-653.

Karous, M., and Hjelt, S. E., 1983. Linear filtering of VLF dip angle measurements: Geophysical Prospecting, **31**, 782-794.

McNeill, J. D., and Labson, V. F., 1991. Geological mapping using VLF radio fields (Ed. Nabighian,M.N.): Electromagnetic Methods in Applied Geophysics, V. 2 Application, Part B, SEG, Tulsa, 521-640.

Ogilvy, R. D., and Lee, A. C., 1991. Interpretation of VLF-EM in-phase data using current density pseudosections: Geophysical Prospecting, **39**, 567-580.

Ogilvy, R. D., Cuadra, A., Jackson, P. D., and Monte, J. L., 1991. Detection of an air-filled drainage gallery by the VLF resistivity method: Geophysical Prospecting, **39**, 845-859.

Paterson, N. R. and Ronka, V., 1971. Five years of surveying with very low frequency electromagnetics method: Geoexploration, **9**, 7-26.

Phillips, W. J., and Richards, W. E., 1975. A study of effectiveness of the VLF method for the location of narrow-mineralised fault zones: Geoexploration, **13**, 215-226.

Tabbagh, A., Benderitter, Y., Andrieux, P., Decriaud, J.P., and Guerin, R., 1991. VLF resistivity mapping and verticalization of the electric field: Geophysical Prospecting, **39**, 1083-1097.